Antal Kerpely Doctoral School of Materials Science and Technology

Evaluation of conventional sintering, induction sintering, and selective laser melting manufacturing procedures of 17-4PH materials

Thesis Booklet

By

Mohammed Qasim Kareem/Yasi

(M.Sc. in Metallurgical Engineering)

Supervisors

Prof. Dr. Zoltan Gacsi, Professor

Dr. Gréta Gergely, Associate Professor

Head of the Doctoral School

Prof. Dr. Valéria Mertinger

Institute of Physical Metallurgy, Metalforming and Nanotechnology

Faculty of Materials and Chemical Engineering

Miskolc, 2025

Table of Contents

1. Introduction

The press and sinter method (PSM) remains the leader in manufacturing ferrous parts among all other powder metallurgical methods worldwide. According to Figure 1(a), the ferrous products obtained through PSM accounted for 63% of the total. A report on the metal powder market size in the United States from 2016 to 2027, which is shown in Figure 1(b), explains the high demand for PSM products compared to additive manufacturing (AM), metal powder injection molding (MIM), and hot isostatic pressing (HIP). The PSM offers low-cost stainless-steel products, net-shaping processing at relatively low sintering temperatures, customised microstructures, beneficial mechanical properties, high surface finishing and dimensional accuracy, and does not cause high pollution [1-7]. To gain perspective on more advantages of PSM, one can compare it with MIM technology. The MIM steel parts are the second most requested method (via sintering route) after the PSM, as shown in Figure 1. However, MIM includes the preparation of the starting material (polymer blend with metal-like properties), injection molding, debinding, and sintering [8-11]. The PSM involves the compaction of the powder (metal or metal alloy, with or without binders), usually in molds, followed by sintering of the molded bodies [6], [7]. The thermal debinding in a high-temperature burnout furnace should be done before sintering in the MIM process, which takes up to 50 hours [4]. In contrast, there is no debinding step in PSM and less periods of sintering cycle. Another advantage of PSM is that the particles bond together directly (without organic materials such as wax), resulting in less oxidation compared with MIM [12].

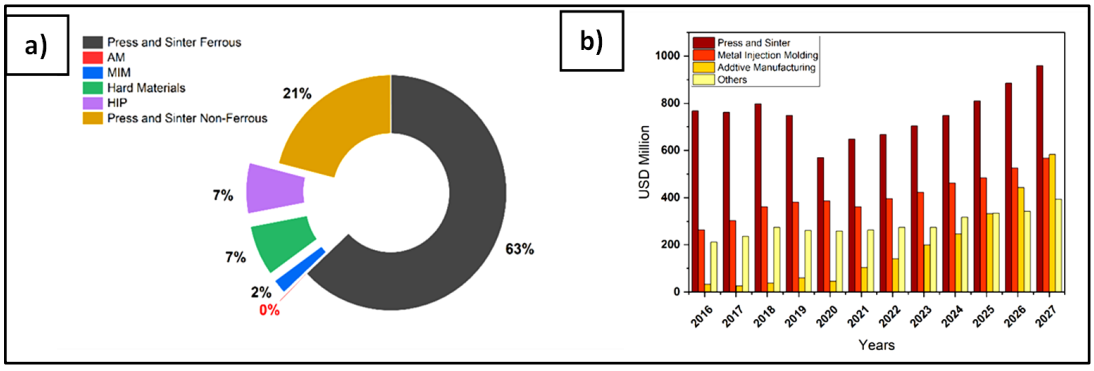

Figure 1.The use of press and sinter technology compared to other processes for producing powdered materials in a) Europe in 2019 and b) the US market over a range of years (according to [13])

17-4PH grade, a precipitation-hardened martensitic stainless steel, has a wide range of applications in the medical, shipbuilding, food, chemical, nuclear, and automotive industries [1], [14-17]. 17-4PH parts are typically used in the aerospace, chemical, petrochemical, and

general metal processing industries [4], [13], [18], [19]. Designers and engineers prefer 17-4PH stainless steel because of its beneficial properties such as high strength, hardness, easy modification by heat treatment, and corrosion resistance at temperatures below 300 °C [19-21]. This is attributed to the alloy containing more chromium and nickel [22], [23]. 17-4PH is usually chosen to produce stainless steel materials with high strength and medium ductility [22], [24]. However, unfortunately, PSM could not previously be used to produce high-density parts from 17-4PH powder due to the poor compressibility of the 17-4PH powder, 17-4PH stainless steel is four times harder than 316L stainless steel [13]. Therefore, few PSM studies were published. The low compressibility of the 17-4PH powder, which leads to low densification, was the main reason for few PSM studies [25-27]. PSM can produce stainless-steel parts with a sintered density of 6.8 to 7.3 g/cm^3 [28]. In contrast, the theoretical density of 17-4PH materials reported in the literature ranges from 7.75 to 7.85 g/cm^3 [29]. However, since both MIM and PSM have similar sintering phenomena, the studies on MIM 17-4PH can be utilised in this dissertation as supportive references.

The main objective of this dissertation is to explore various factors influencing challenges in the production of PSM 17-4PH parts. These factors included applying high cold pressing, utilising conventional and induction furnaces for low and high sintering temperatures, and sintering for various short and long times. Additionally, these investigations performed, for the first time, using gas-atomised instead of water-atomised 17-4PH powder, the water-atomised 17-4PH powder is common for PSM 17-4PH parts. Moreover, the impact of decreasing the 17-4PH powder particle size on the densification property and recyclability of 17-4PH from the 3D printing process to produce PSM 17-4PH parts were investigated as well. Conversely, various key parameters of the selective laser melting (SLM) method were analysed to create high-density SLM 17-4PH components. Lastly, a heat-treatment condition was applied to compare the physical-mechanical properties of 17-4PH parts produced by sintering and melting routes. A comprehensive review of the literature was conducted, highlighting the existing knowledge gap. Objectives were established, experiments were designed, conducted, and evaluated scientifically, and subsequently presented for consistency.

2. Scientific questions

The following points outline the scientific questions that could not be addressed previously according to the reported literature:

1) 760 MPa was the maximum cold pressing used to produce PSM 17-4PH parts. Applying a higher cold pressing than what was used in the literature needs to be investigated. Additionally, gas-atomised powder had not been previously utilised in the production of PSM 17-4PH parts. There is an interesting scientific question regarding whether the use of gas-atomised powder instead of water-atomised powder is applicable.
2) The literature indicates that using a sintering temperature below 1220 °C for producing PSM 17-4PH parts is not advisable due to the risk of incomplete sintering. At the same time, a lower sintering temperature decreases the shrinkage value, which is beneficial for the technical manufacturers as it preserves the product dimensions. Therefore, how can high cold pressing improve the application of the low sintering temperature of 1200 °C in the production of stainless-steel PSM parts with satisfactory physical-mechanical properties?
3) The average smallest particle size of the 17-4PH powder reported in the literature is 45 μm. Therefore, clarifying how a reduction in particle size affects the porosity of the PSM 17-4PH parts appears to address a gap. Furthermore, the literature indicates that there has been no prior use of 17-4PH powder from the 3D printing process to produce PSM 17-4PH parts. Consequently, an open question remains regarding the recyclability of this powder.
4) No study has yet examined the impact of using induction heating sources in the sintering process of 17-4PH parts, along with their densification and mechanical properties. Therefore, how does the induction heating source reduce the required sintering time and enhance the physical-mechanical characteristics of induction sintering (INDS) 17-4PH samples?
5) Avoiding scan voids is a critical issue due to its direct connection to SLM machine-type standards. This problem affects the density reduction (and lower mechanical properties) of SLM 17-4PH samples. How can we assess various parameters (energy density, scanning strategy, and fixed contour value) during 3D printing using the SLM method to eliminate actual porosity (subsurface pores)? Which approach can achieve the highest density and improve strength properties?
6) Comparing the physical-mechanical properties of 17-4PH samples produced by various methods poses a significant challenge and has not been previously explored. However, applying a heat-treatment condition (H900) can aid in the comparison process. Moreover, heat treatment is a primary procedure for the stainless-steel part

before its deployment. Consequently, how would the implementation of H900 influence the physical-mechanical properties of 17-4PH produced using various techniques: conventional sintering, induction sintering, and additive manufacturing (via SLM)? Furthermore, is the comparative approach relevant?

3. Materials and methods

3.1 Stainless-steel powders used in this research work

The following list presents the stainless-steel materials utilised in this dissertation work:

1- Original powder was the as-received Oerlikon gas-atomised 17-4PH powder. This powder had a particle size distribution ranging from 15 to 45 µm.

2- The recycled powder is the original 17-4PH after using several time in producing 3D 17-4PH components.

3.2 Preparation procedures

The preparation procedures of the investigated samples can be summarized in figures with all essential details. The DCTT code refers to the samples manufactured from original 17-4PH powder using PSM method at different cold pressing, sintering temperature, and sintering times. The preparation steps of the DCTT samples are presented in Figure 2. The value of 10 °C/min was the heating rate and cooling rate.

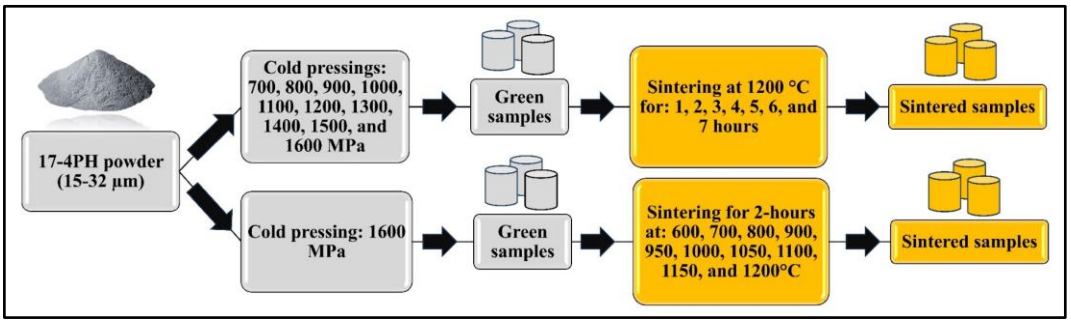

Figure 2.The manufacturing procedures for DCTT 17-4PH samples.

The O and R samples refer to 17-4PH samples manufactured from original and recycled powders, respectively. The diagram illustrating the manufacturing steps is shown in Figure 3.

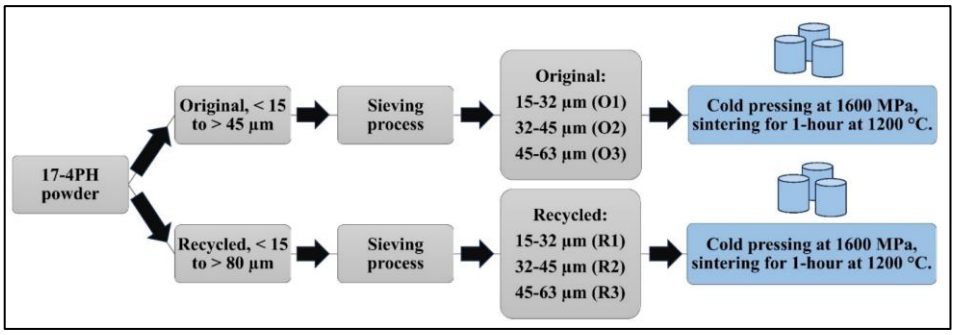

Figure 3.Illustrates the original and recycled 17-4PH samples manufacturing steps.

The INDS samples refer to the samples manufacturing using induction sintering process. The heating and cooling rate through induction furnace are 100 and 60 °C/min, respectively. The manufacturing procedures are detailed in Figure 12.

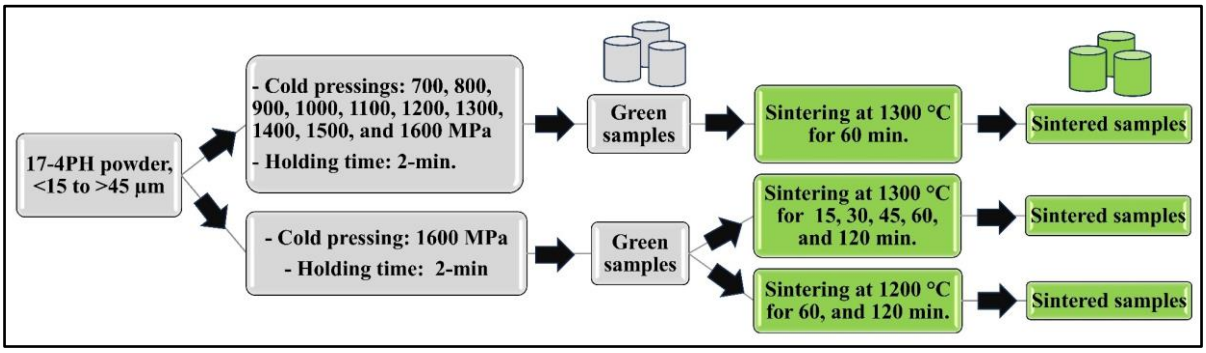

Figure 4.Manufacturing procedures of INDS 17-4PH samples.

The SLM samples refer to the samples manufactured from recycled 17-4PH powder using a selective laser melting method. The SLM process comprises two distinct manufacturing setups designated as 1SLM and 2SLM, which are detailed in Table 2. The normal and zigzag strategies are illustrated in Figure 5.

Table 1.Represents the SLM method designed setups**.**

Samples code / Parameters	1SLM	2SLM
Laser Power, W	107	168
Laser Speed, mm/s	1200	1000
Layer thickness, µm	25	35
Hatch distance	100	
Energy Density, J/mm²	36	48
Scan Strategy	Normal with 45° rotation	Zigzag with 45° rotation
Contour	2	
Sample Orientation	45°	
Space between contour and hatch	0	
Beam diameter	40 µm	
Shield gas	nitrogen	

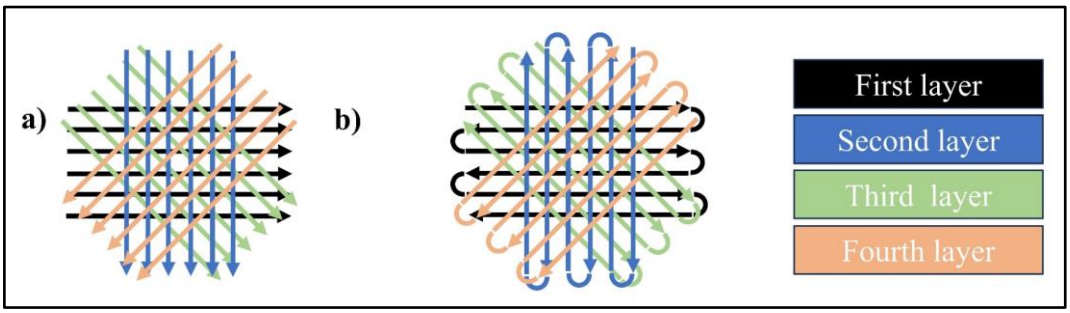

Figure 5.Examples of the 45° rotating of a) normal, and b) zigzag scanning strategies.

The HT-CPCS, HT-INDS, and HT-SLM refer to the samples manufactured using conventional sintering (manufacturing conditions: 1600 MPa, sintered at 1300 °C for 1-h), induction sintering (manufacturing conditions: 1600 MPa, sintered at 1300 °C for 1-h), and SLM (48 J/mm^2 and zigzag scan strategy) after applying a heat-treatment condition call H900, as presented in table 3. The H900 procedure involves solution heat treatment (annealing) at 1038 °C for 30 minutes in an argon atmosphere, followed by quenching in water. The annealed samples were then aged at 480 °C for 60 minutes in an argon atmosphere. The heating rate during the annealing and aging treatments was 10 °C/min.

Table 2. Coding of the heat treated 17-4PH samples produced by PSM, INDS, and SLM methods.

Method	Conventional sintering	Induction sintering	Selective laser melting
Code	HT-CPCS	HT-INDS	HT-SLM

3.3 Measurements

Dimensional and Archimedes methods were utilised for density measurements. To understand the thermal behavior of the original PSM 17-4PH samples, a differential scanning calorimetry (DSC) test was conducted. The phase compositions of the manufactured 17-4PH samples were characterized using X-ray diffraction (XRD) and electron backscatter diffraction (EBSD). The cross-sections of the manufactured samples were examined through optical microscopy, scanning electron microscopy (SEM), energy dispersive spectroscopy (EDS), and focused ion beam (FIB)-SEM analysis. ImageJ software was employed to analyse the cross-sectioned microstructures. The Vickers hardness was measured with a 10 kg load on both the cross-sectional and top surfaces of selected samples. To assess the mechanical properties of the manufactured samples in this research, the compressive strength was evaluated using the same cold pressing machine (the universal tensile testing

equipment) at room temperature, with a maximum load of 10 tons. Three samples were the minimum number of parallel samples to enhance the measurements.

4 Claims

Claim 1. Achieving high relative green (~ 92%) and sinter density (~ 98%) and minimal volume shrinkage of PSM 17-4PH materials (5.53%)

a.1 The relative green density increased from 80.20 ± 0.28 to 91.76 ± 0.18 % as the application of cold pressing rose from 800 MPa to 1600 MPa, see Figures C1.1 and C1.2. The application of 1600 MPa improved the relative green density by approximately 11% compared to the reported literature.

b.1 Seven hours of sintering time at electric sintering temperatures of 1200 °C improved the relative sinter density of the DCTT 17-4PH samples to approximately 98% (see Figure C1.2), which is 4% higher than what is reported in the literature with significantly higher sintering temperatures. It is important to note that 1260 °C was the minimum sintering temperature mentioned in the literature. The DCTT samples demonstrated a lower volume shrinkage of 5.53% (see Figure C1.3), which is 46% less than the reported literature. This reduction resulted from reducing the difference between relative green and sinter densities, as well as applying a relatively low sintering temperature of 1200 °C.

c.1 The linear regression equation, as indicated below and in Figure C1.2, can predict the relative sinter density of the DCTT 17-4PH samples based on various sintering times (from 0 to 7 hours) at 1600 MPa and 1200 °C. The linear regression equation: $y = 0.81x + 93.22$; y: relative sinter density by %; x: sintering time by hour.

d.1 The seven hours of sintering significantly lowered the γ-content to 0.12%, while the α/ά-content increased, as illustrated in Figure C1.4. The increase in BCC amount is linked to the α-phase, which decreased the porosity. Consequently, the DCTT samples (which were cold pressed at 1600 MPa and sintered at 1200 °C for seven hours) achieved a higher HV (around 43%) and improved strength (approximately 10%) compared to the literature.

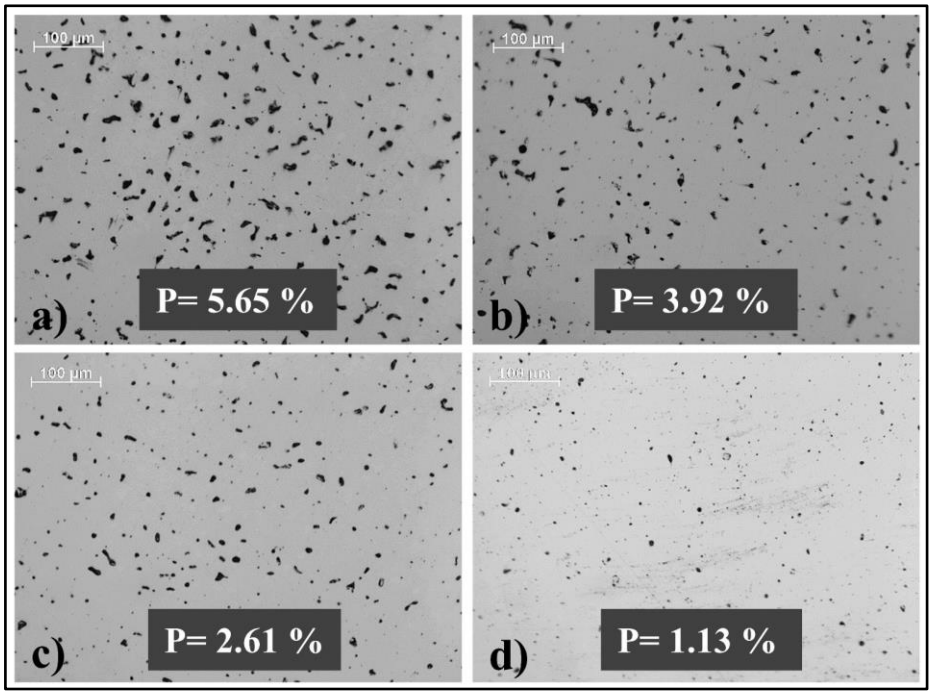

Figure C1.1. The impact of cold pressing on the optical microscopic ImageJ porosity of DCTT 17-4PH samples cold pressed at a) 800 MPa, b) 1000 MPa, c) 1200 MPa, and d) 1600 MPa after seven hours of sintering at 1200 °C.

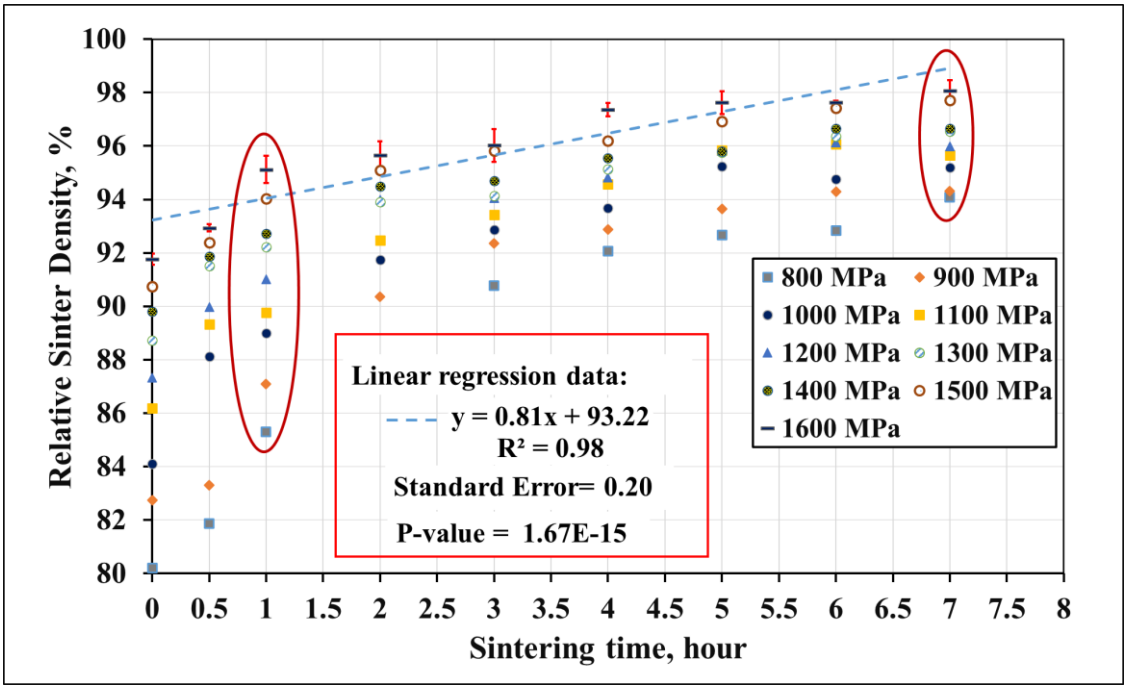

Figure C1.2 The impact of cold pressing and sintering time on the relative sinter densities of DCTT 17-4PH samples, sintered at 1200 °C.

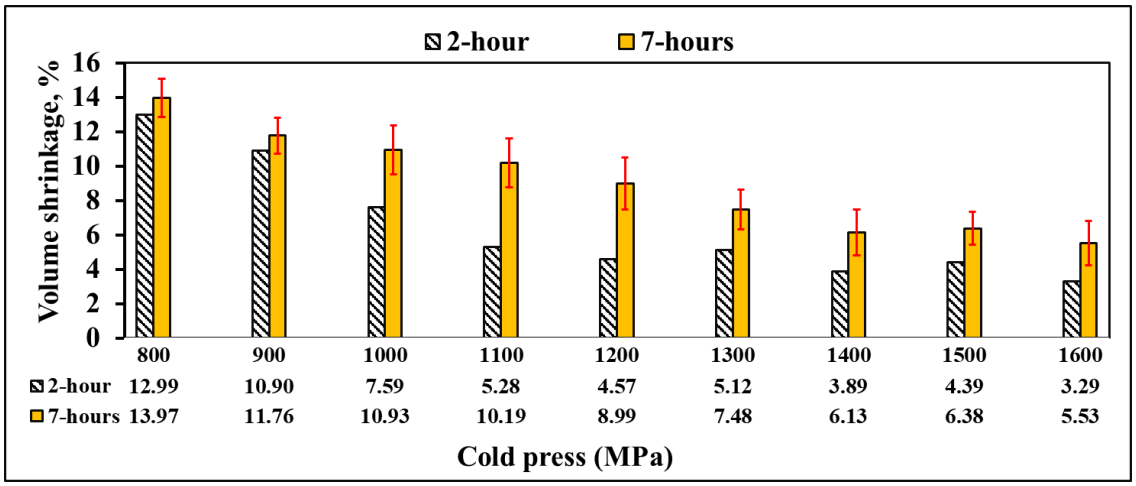

Figure C1.3. Volume shrinkage of selected DCTT 17-4PH samples sintered at 1200 °C for different times.

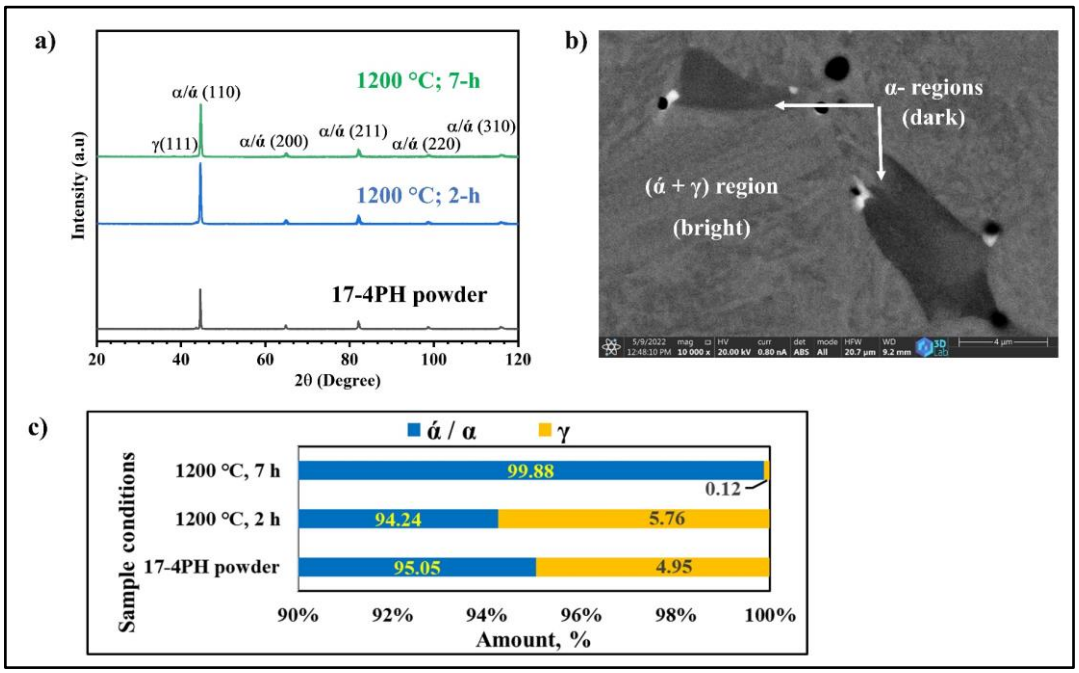

Figure C1.4. Illustrates a) the XRD diffractograms, b) the FIB-SEM image, and c) the phase amounts of DCTT 17-4PH samples. Note: The FIB-SEM image corresponds to a DCTT sample sintered at 1200 °C for two hours.

Claim 2. The recycled 17-4PH samples demonstrated a slightly higher strength (R1 with 923 MPa) compared to the original samples (O1 with 917 MPa), which can be considered negligible.

The recycled (reused multiple times in the production of 3D printed parts using SLM) 17-4PH powder contained fused and welded particles, which are absent in the original 17-4PH powder. The recycled PSM 17-4PH samples exhibited a larger pore area (approximately double) compared to the original samples, as illustrated in Figure C2.1. The carbon content

of the recycled 17-4PH powder (0.02%) was slightly higher than that of the original powder (0.01%). This was noted in recycled samples with a marginally increased martensitic content, as depicted in Figure C2.2. Consequently, the analyses of the recycled samples (with the lowest particle size distribution of 15–32 µm) demonstrated a slightly higher strength (R1 with 923 MPa) compared to the original samples (O1 with 917 MPa), which can be considered negligible.

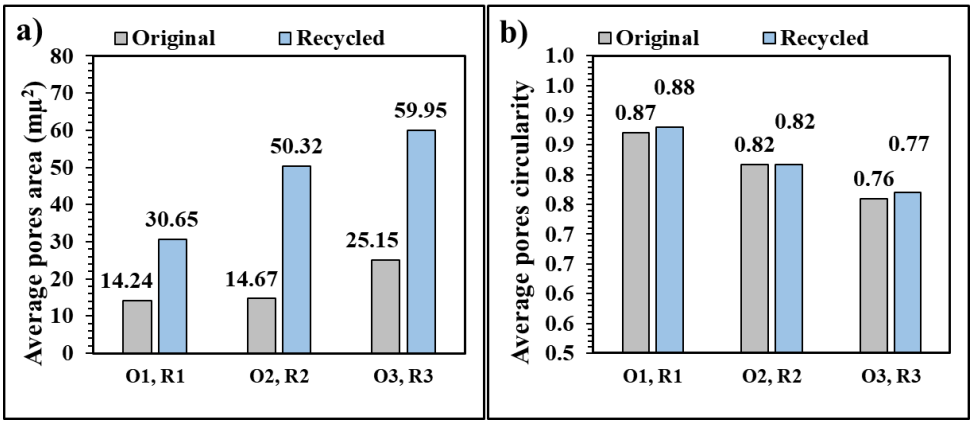

Figure C2.1. Represents a) average pores area, and b) pores circularity by ImageJ of unetched original and recycled samples.

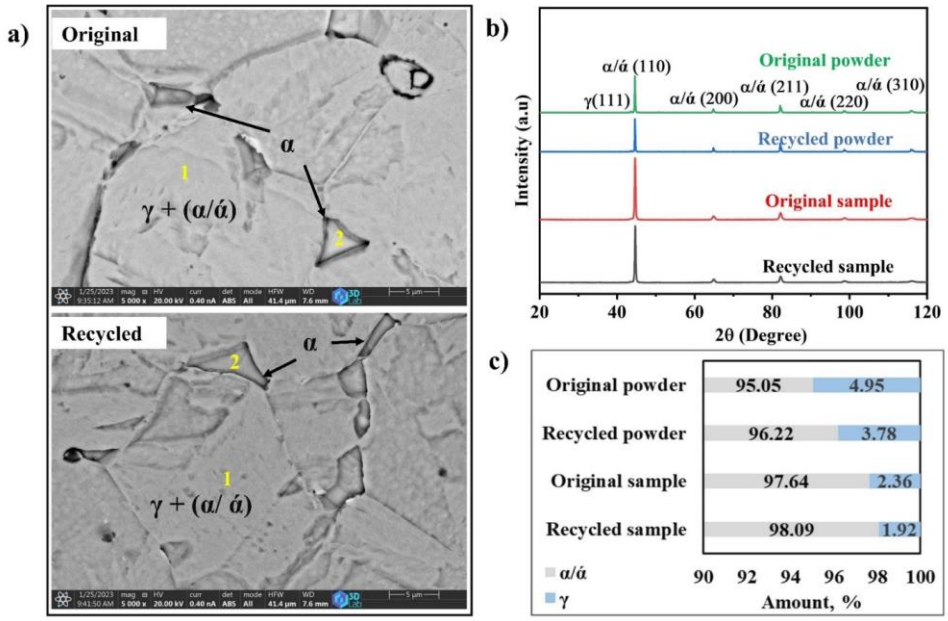

Figure C2.2. Phases approved by a) Backscattered-SEM images, b) XRD pattern, and c) XRD phases volume fraction of original and recycled samples.

Claim 3. Induction sintering produced 17-4PH parts with ~99% relative density after 1-hour of sintering instead of 7-hours by electrical sintering

a.3 Instead of long sintering time of seven hours using electrical furnaces in claim 1, induction furnace could achieve around 99% as a relative sinter density of INDS 17-4PH materials in one hour and at sintering temperature of 1300 °C. Sintering at 1200

°C, using induction furnace, led to incomplete of sintering and high porosity. The impact of cold pressing on enhancing relative sinter densities (by increasing relative green densities) was less pronounced in the case of induction sintering compared to electrical sintering (claim 1). The induction sinter density increased 3% with increasing cold pressing from 700 to 1600 MPa, 3% with increasing sintering temperature from 1200 to 1300 °C, and 1% with increasing sintering time from 15 to 120 minutes (see Figure C3.1). There was no noticeable difference between the density of samples sintered at one and two hours. But 120 minutes caused over coarsening, see Figures C3.2.

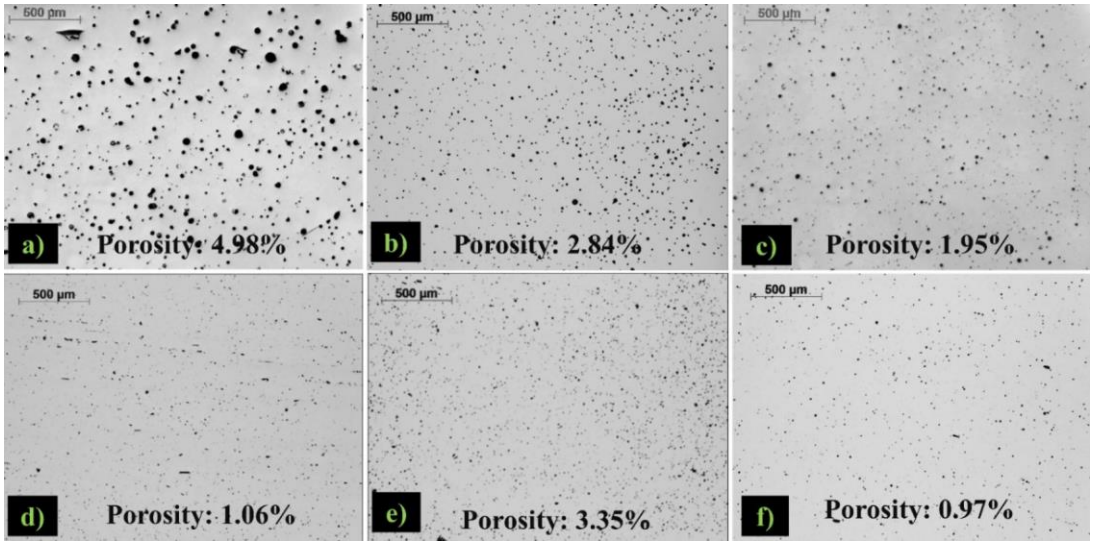

Figure C3.1. The ImageJ porosity 17-4PH optical microstructures manufactured at a) 1300 °C for 60 min at 700 MPa, b) 1300 °C for 60 min at 1000 MPa, c) 1300 °C for 15 min at 1600 MPa, d) 1300 °C for 60 min at 1600 MPa, e) 1200 °C for 120 min at 1600 MPa, and f) 1300 °C for 120 min at 1600 MPa.

b.3 The Cu did not evaporate during induction sintering; however, it diffused alongside the formation of δ-ferrite. The Cu-content in the α-region decreased with rising sintering temperature and times, see Figure C3.2 (h). The Cu wt.% decreased by approximately 32% in α-region compared to ά+γ-region at 1300 °C for 60 minutes. This decrement ratio decreased with a reduction in sintering time (15 minutes at 1300 °C) to 16%, and to 27% with a decrease in sintering temperature to 1200 °C for 120 minutes. Conversely, it increased to 46% with an increase in sintering time to 120 minutes at 1300 °C.

c.3 The FCC (γ-phase) increased from 5% to 13% with increasing sintering times from 15 to 120 minutes, see Figure C3.3. The amount of untransformed γ-phase (which can be retained austenite) after cooling is closely related to its amount during heating,

influenced by the sintering times at 1300 °C. This might cause a decrease in strength properties during service due to the transformation to induced martensite.

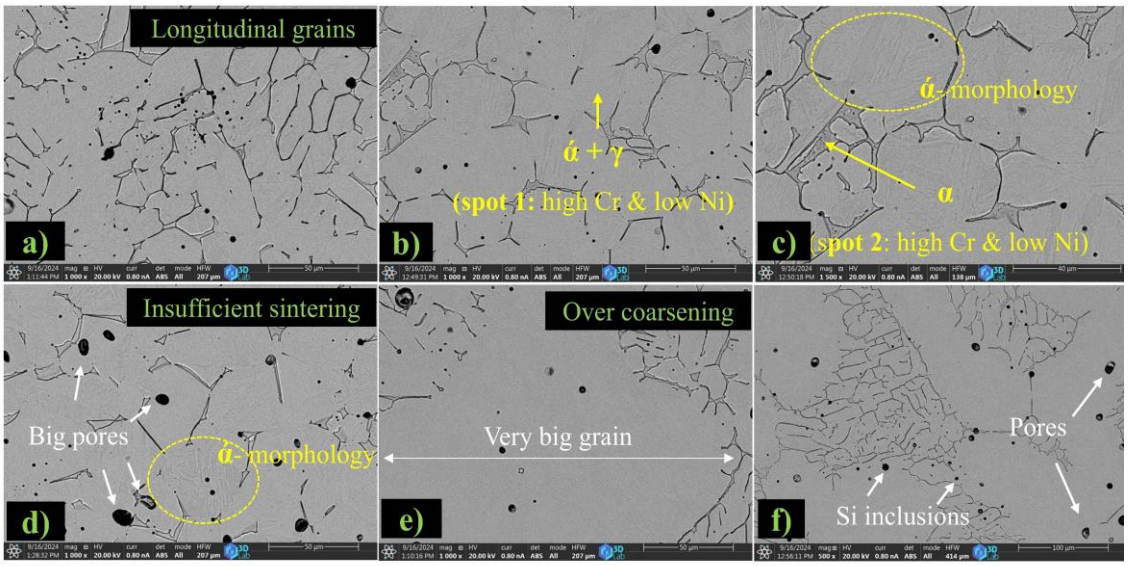

g)

Element by EDS	O K	SiK	MoL	CrK	FeK	NiK	CuK
Weight % (spot 1)	1.37	0.37	0.16	15.95	74.18	4.25	3.71
Weight % (spot 2)	1.43	0.44	0.23	22.34	70.57	2.45	2.54

h)

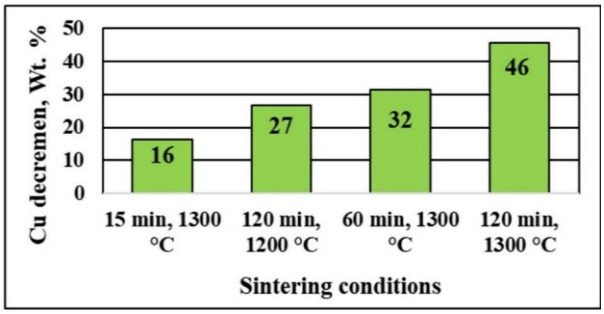

Figure C3.2. The SEM images and EDS analyses of INDS 17-4PH samples cold pressed at 1600 MPa and sintered at a) 1300 °C, 15 min., b and c) 1300 °C, 60-min (different magnifications), d) 1200 °C, 120-min, e and f) 1300 °C, 120-min (different magnifications). The EDS analyses of the spots in (c and b) are presented in (g). EDS Cu-decrement is presented in (h).

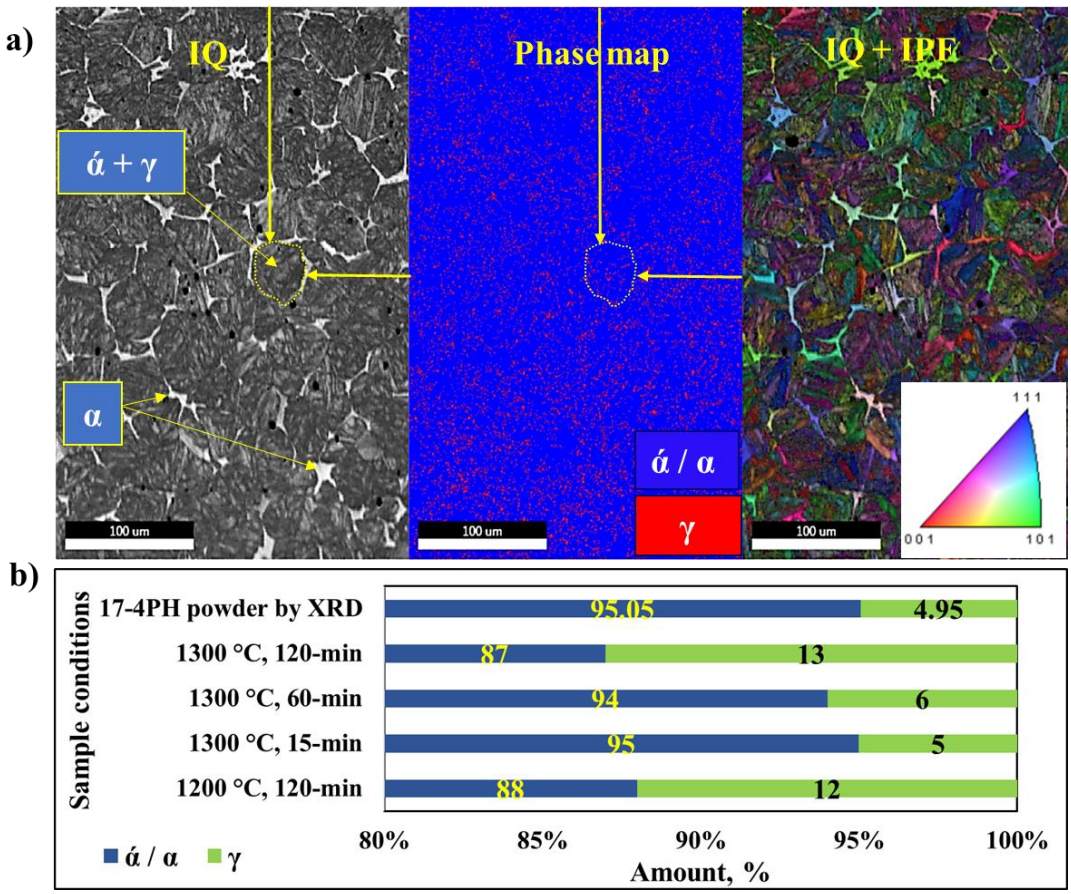

Figure C3.3. EBSD analysis results of (a) the IQ image and IPF map, and (b) the phases percentages of 17-4PH sample for cold pressed at 1600 MPa and sintered for 60 min.

Claim 4. Diminish scan voids and produce SLM 17-4PH parts with extremely high density and high mechanical properties

The zigzag scanning strategy and selecting appropriate energy density (48 J/mm^2) was sufficient to eliminate scan voids (see Figures C4.1 and C4.2) without altering the contour values and reducing the space between hatch scan tracks and contour tracks, as recommended by the literature. Utilising post-processing to remove the first voids shell from an SLM17-4PH sample may be considered unnecessary due to this achievement. However, in comparison to the literature, this work achieved an improvement in the HV value of over 5%, with a high compressive yield strength reaching 818 MPa.

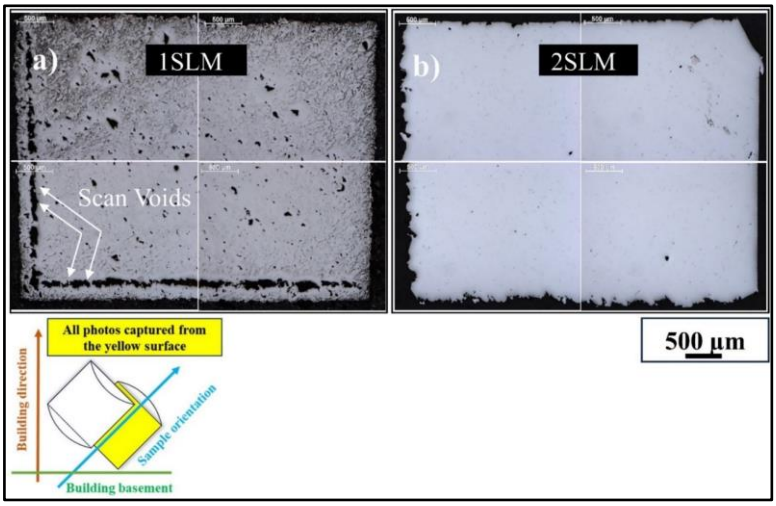

Figure C4.1. Illustrates the effect of the scan strategy on the formation of scan voids on the sectional surfaces of a) 1SLM, and b) 2SLM.

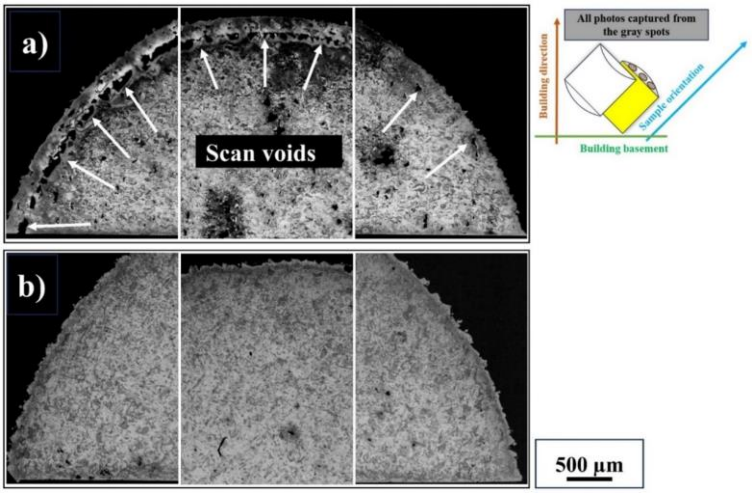

Figure C4.2. The effect of the scan strategy on the formation of scan voids on the top surfaces of a) 1SLM and b) 2SLM samples

Claim 5. Comparing between 17-4PH samples produced by conventional and induction sintering, and SLM methods by applying H900 condition

a.5 The γ-amount increased by approximately 3% in the HT-SLM compared to both HT-CPCS and HT-INDS samples (see Figure C5.1). This may be attributed to the higher carbon content in the recycled 17-4PH powder and the formation of retained austenite. The increase in γ-amounts after the application of H900 compared to the states before H900 may be attributed to the solution heat treatment.

b.5 The final relative densities of the HT-INDS and HT-SLM samples were 98.79% and 98.85%, respectively. According to the SEM results (see Figure C5.2), the α-regions are larger in the HT-INDS case compared to the HT-CPCS, but are absent in the HT-SLM samples. The grain size distributions of the HT-SLM sample were the smallest compared to both HT-CPCS and HT-INDS samples. The tops of the area fractions intersect with

their grain sizes of approximately 5 µm, 6 m, and 10 m for HT-SLM, HT-CPCS, and HT-INDS samples. This confirmed by refined SEM microstructure of the HT-SLM sample, see Figure C5.2. All of the factors mentioned resulted in a lower HV for the HT-INDS (397) compared to that of HT-SLM (448), despite their similar densification values. The compressive yield strength, see Figure C5.3, of the HT-SLM was significantly higher (1442 MPa) than that of the HT-INDS samples (1218 MPa).

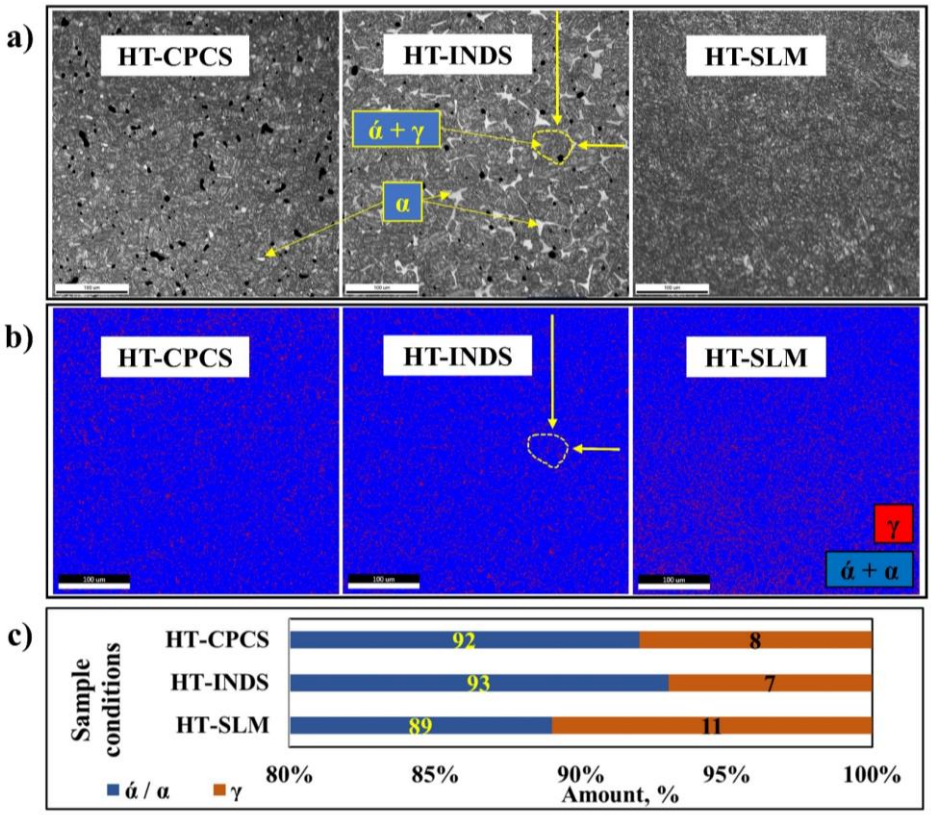

Figure C5.1. Showes a) the IQ+IPF images, b) the phases distributions, and c) the phases percentages of heat-treated 17-4PH samples.

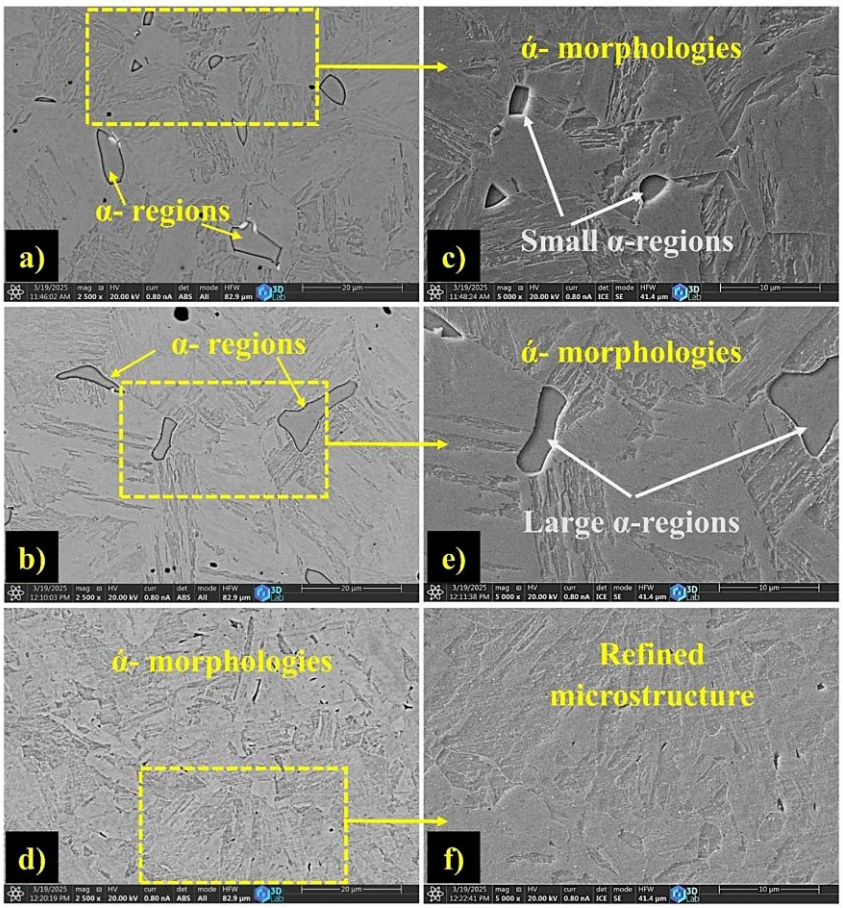

Figure C5.2. The SEM images of a) HT-CPCS, b) HT-INDS, and d) HT-SLM samples. c), e), and f) refer for the SE mode and higher magnifications of a), b), and d), recpectively.

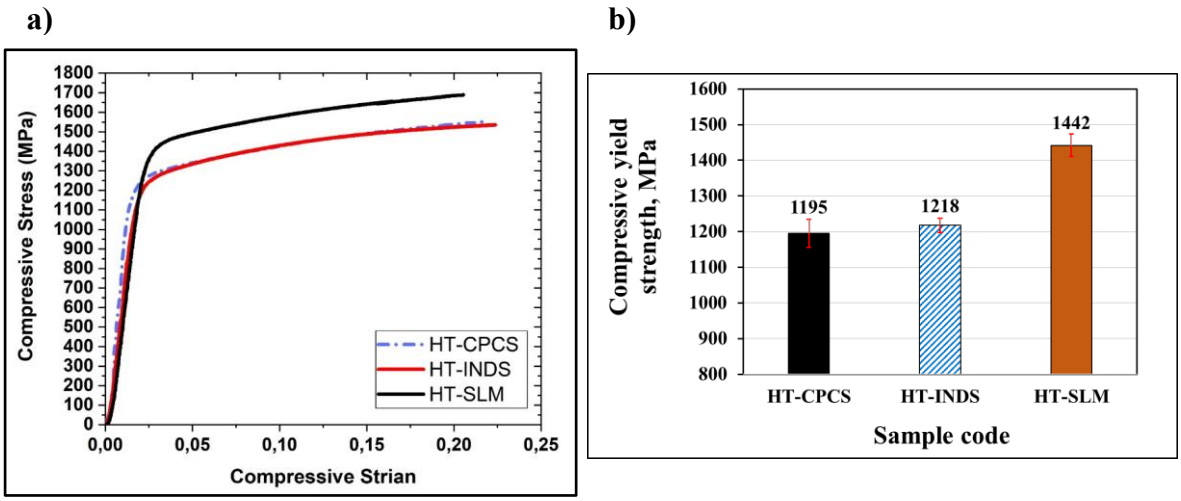

Figure C5.3. Represents a) the stress-strain curves, b) the strength of all heat-treated 17-4PH samples

5. Summary

The existing literature reveals a lack of sufficient studies focused on enhancing the inadequate densification of PSM 17-4PH parts, as the high porosity of these pats remains the primary obstacle to their application. Additionally, the critical PSM parameters encompass cold pressing, sintering temperatures, and sintering durations, all of which significantly influence the density and the physical and mechanical properties of PSM 17-4PH parts. Therefore, this dissertation work presents a thorough analysis of the aforementioned parameters. In addition, different furnaces with different heating resources (electrical and induction) are employed to produce PSM 17-4PH parts. Additionally, literature has reported no studies comparing the physical-mechanical characteristics of various methods for producing 17-4PH parts. The market still favors PSM parts over newer technologies like SLM parts, primarily due to the cost-effectiveness of PSM stainless steel components. However, in terms of physical-mechanical properties, SLM 17-4PH parts are preferred over PSM 17-4PH parts because of the lower density of the latter. This study utilised a heat-treatment process as a necessary step prior to export for actual service conditions, aiming to compare the physical and mechanical properties of 17-4PH parts produced by various techniques, primarily PSM and SLM.

This work achieves, for the first time, compelling comparisons between different manufacturing methods of 17-4PH powdered materials. It revitalizes PSM technology, enabling the production of 17-4PH parts using relatively low sintering temperatures (1200 °C, economical) to achieve a high densification of 17-4PH product (98%). Conversely, 1260 °C was the minimum sintering temperature and could not increase density beyond 93% (as noted in the literature section of this dissertation). The PSM in this dissertation reduced shrinkage by 46% compared to the literature, which lowers the cost of post-processing by maintaining the dimensions of the final product nearly identical to their initial state (before sintering). Additionally, for the first time, induction sintering was applied in this dissertation work, successfully increasing the relative sinter density to around 99% in just one hour at 1300 °C. These achievements provide manufacturers with greater flexibility in choosing a manufacturing method over MIM and SLM, which are considered more expensive than press and sinter routes.

6. Author publications in the subject of the thesis

6.1 Journal paper

1- Kareem, Mohammed Qasim; Mikó, Tamás; Gergely, Gréta; Gácsi, Zoltán. A review on the production of 17-4PH parts using press and sinter technology. SCIENCE PROGRESS, 106: 1Paper: 003685042211460, 31 p. (2023). Independent citation: 4, *Journal Rank: Q1*

2- Kareem, Mohammed Qasim; Mikó, Tamás; Gergely, Gréta; Gácsi, Zoltán. Compaction behaviours of 17-4 PH, 316L, and 1.4551 stainless-steel powders during cold pressing. RESULTS IN ENGINEERING, 23: 102452, 8 p. (2024). Independent citation: 1, Journal *Rank: Q1*

3- Kareem, Mohammed Qasim; Mikó, Tamás; Gergely, Gréta; Gácsi, Zoltán. Optimisation of Powder Metallurgy Technology of 17-4PH Material. HELIYON, 11: 4: e42658, 15 p. (2025). *Journal Rank: Q1*

4- Mohammed, Qasim Kareem; Tamás, Mikó; Gréta, Gergely; Zoltán, Gácsi Choosing an Appropriate Additive Manufacturing Method for Printing 3D 17-4PH Parts: A Review. DOKTORANDUSZ ALMANACH.1, pp. 336-343., 8 p. (2022). Publication:33541234 Published Core Journal Article (Article) Scientific.

5- Kareem, Mohammed Qasim; Mikó, Tamás; Dávid Halápi; Gergely, Gréta; Gácsi, Zoltán. Employing Recycled 17-4PH Powder to Produce Press and Sinter Parts with Adequate Physical-Mechanical Properties. Submitted to RESULTS IN MATERIALS, *Journal Rank: Q2.*

6.2 Conference presentations

1. Mohammed, Qasim Kareem; Tamás, Mikó; Gréta, Gergely; Zoltán, Gácsi. Producing Cost-Effective Sintered 17-4ph Materials with High Physical and Mechanical Properties. The 17th Miklós Iványi International PhD and DLA Symposium 25-26 Oct 2021, Pécs, Hungary.
2. Mohammed, Qasim Kareem; Tamás, Mikó; Gréta, Gergely; Zoltán, Gácsi. The effect of applying massive cold pressing through conventional powder metallurgy on density of different stainless-steels compacts. In: Gökhan, GÜNDÜZ (eds.) Mediterranean International Conference on Research in Applied Sciences: The proceedings book Ankara, Turkey: İksad Yayınevi(2022) p. 62, Publication:33540745.
3. Mohammed, Qasim Kareem; Tamás, Mikó; Gréta, Gergely; Zoltán, Gácsi. Effect of Cold Pressing, Sintering Time, and Sintering Temperature on Densification of Press and Sintered 17-4PH Materials. (2022) microCAD Nemzetközi Multidiszciplináris Tudományos Konferencia 2022-10-13, Publication:33540797.
4. Mohammed, Qasim Kareem; Tamás, Mikó; Gréta, Gergely; Zoltán, Gácsi. Investigations of pressed and sintered components using 17-4PH powder collected in the chamber of an SLM printer Participated at the 23rd Annual Conference on Material Science -YUCOMAT 2022 which was held from 29.08 - 02.09.2022. in Herceg Novi, Montenegro, with Oral Presentation.
5. Mohammed, Qasim Kareem; Tamás, Mikó; Gréta, Gergely; Zoltán, Gácsi. Manufacturing of 17-4PH SLM Parts with Different Scanning Angles and Sample Orientations. Book of Abstracts from 9th International Scientific Conference on Advances in Mechanical engineering.Scientific Books of Abstracts, Vol. 2, pp 47-47 © 2023 Trans Tech Publications Ltd, Switzerland.

References

[1]-Ali S, Rani AM, Altaf K, Baig Z. Investigation of Boron addition and compaction pressure on the compactibility, densification and microhardness of 316L Stainless Steel. IOP conference series: materials science and engineering 344(1), 012023 (2018). doi:10.1088/1757-899X/344/1/012023

[2]-Acar AN, Ekşi AK, Ekicibil A. Effect of pressure on the magnetic and structural properties of X2CrNiMo17-12-2 austenitic stainless steel prepared by powder metallurgy method. Journal of Molecular Structure 15, 1198, 126876 (2019). doi:10.1016/j.molstruc.2019.126876

[3]-Kareem MQ, Dorofeyev V. Effect of fullerenes additions on physical–mechanical properties of hot-forged iron-based powder materials. IOP Conference Series: Earth and Environmental Science 877 (1), 012009 (2021). doi.org/10.1088/1755-1315/877/1/012009

[4]-R. Schroeder, G. Hammes, C. Binder, and A. N. Klein. Plasma Debinding and Sintering of Metal Injection Moulded 17-4PH stainless steel. Materials Research, 14 (4), 564–568 (2011). doi:10.1590/S1516-14392011005000082.

[5]- Bai, Yu, Lei Li, Leijie Fu, and Qiangfeng Wang. A review on high velocity compaction mechanism of powder metallurgy. Science Progress, 104 (2), 1–20 (2021). doi: 10.1177/00368504211016945.

[6]-B. Kozub, J. Kazior, and A. Szewczyk-Nykiel. Sintering kinetics of austenitic stainless steel aisi 316l modified with nanographite particles with highly developed bet specific surface area. Materials, 13 (20), 1–21 (2020). doi: 10.3390/ma13204569.

[7]-Cristofolini, Ilaria, A. Rao, Cinzia Menapace, and Alberto Molinari. Influence of sintering temperature on the shrinkage and geometrical characteristics of steel parts produced by powder metallurgy. Journal of Materials Processing Technology 210 (13), 1716-1725 (2010). doi:10.1016/j.jmatprotec.2010.06.002

[8]-S. Altıparmak, V. Yardley, Z. Shi, J. L.-I. J. of, and undefined 2020. Challenges in Additive Manufacturing of High-Strength Aluminium Alloys and Current Developments in Hybrid Additive Manufacturing. International Journal of Lightweight Materials and Manufacture, 4 (2), 246-261(2021).

[9]-Wu Y, German RM, Blaine D, Marx B, Schlaefer C. Effects of residual carbon content on sintering shrinkage, microstructure and mechanical properties of injection molded 17-4 PH stainless steel. Journal of materials science, 37, 3573-83 (2002). doi:10.1023/A:1016532418920

[10]-G. Singh, J. M. Missiaen, D. Bouvard, and J. M. Chaix. Additive manufacturing of 17–4 PH steel using metal injection molding feedstock: Analysis of 3D extrusion printing, debinding and sintering. Addit Manuf, 47, (2021).doi:10.1016/j.addma.2021.102287.

[11]-Zaky MT, Soliman FS and Farag AS. Influence of paraffin wax characteristics on the formulation of wax-based binders and their debinding from green molded parts using two comparative techniques. J Mater Process Technol, 209, 5981–5989 (2009).

[12]-H. Ye, X. Y. Liu, H. Hong. Sintering of 17-4PH stainless steel feedstock for metal injection molding. Materials Letters, 62(19), 3334–3336 (2008). doi: 10.1016/J.MATLET.2008.03.027

[13]-M. Q. Kareem, T. Mikó, G. Gergely, and Z. Gácsi. A review on the production of 17-4PH parts using press and sinter technology. Science Progress, 106 (1), (2023). doi: 10.1177/00368504221146060

[14]-Serafini FL, Peruzzo M, Krindges I, Ordoñez MF, Rodrigues D, Souza RM, Farias MC. Microstructure and mechanical behavior of 316L liquid phase sintered stainless steel with boron addition. Materials Characterization, 152, 253-64 (2019). doi: 10.1016/j.matchar.2019.04.009

[15]-Ertugrul O, Park HS, Onel K, W-P. M. Effect of particle size and heating rate in microwave sintering of 316L stainless steel. Powder Technology, 253,703-9 (2014). doi:10.1016/j.powtec.2013.12.043

[16]-Oh JW, Ryu SK, Lee WS, Park SJ. Analysis of compaction and sintering behavior of 316L stainless steel nano/micro bimodal powder. Powder Technology 322, 1-8 (2017). doi:10.1016/j.powtec.2017.08.055

[17]-Giganto S, Martínez-Pellitero S, Barreiro J, Zapico P. Influence of 17-4 PH stainless steel powder recycling on properties of SLM additive manufactured parts. Journal of Materials Research and Technology, 16, 1647-58 (2022). doi: 10.1016/j.jmrt.2021.12.089

[18]-Mohammad Moradi J, Emadoddin E and Omidvar H. Transient liquid phase bonding of 17-4-ph stainless steel using conventional and two-step heating process. Met Mater Int, 27, 5268–5277 (2020).
[19]-Zhang H. Powder injection molding of 17-4ph stainless steel. In: Metal Powder Industries Federation (ed) Powder injection molding symposium, 219–227 (1992).
[20]-Szewczyk-Nykiel A. The effect of the addition of boron on the densification, microstructure and properties of sintered 17-4 PH stainless steel. Technical Transactions Mechanics. In: Czasopismo Techniczne, 86–96 (2014).
[21]-Wang FZ, Wang QZ, Yu BH, et al. Interface structure and mechanical properties of Ti (C, N)-based cermet and 17–4PH stainless steel joint brazed with nickel-base filler metal BNi-2. J Mater Process Technol, 211, 1804–1809 (2011).
[22]-Patibandla AR. Effect of process parameters on surface roughness and porosity of direct metal laser sintered metals. Master thesis, University of Cincinnati, Cincinnati, USA, 2018.
[23]-Samal PK, Nandivada N, Hauer I, et al. Properties of 17-4ph stainless steel produced via press and sinter route. Adv Powder Metallurg Particulat Mater 2008; 7: 109–120.
[24]-Kazior J, Szewczyk-Nykiel A, Pieczonka T, Hebda M, Nykiel M. Properties of precipitation hardening 17-4 PH stainless steel manufactured by powder metallurgy technology. Advanced Materials Research 811, 87-92 (2013). doi: 10.4028/www.scientific.net/AMR.811.87
[25]-C.T. Schade, P.D. Stears, A. Lawley, R.D. Doherty. Precipitation-hardening PM stainless steels. International Journal of Powder Metallurgy, 43(4) (2007).
[26]-H. Irrinki. Mechanical properties and microstructure evolution of 17-4 PH stainless steel processed by laser-powered bed fusion. Master thesis, University of Louisville, 2016. doi:10.18297/etd/2408
[27]-S. Dobson, S. Vunnam, D. Frankel, C. Sudbrack, T. Starr. Powder variation and mechanical properties for SLM 17-4 PH stainless steel. in: International Solid Freeform Fabrication Symposium, University of Texas, Austin, United State of America, 2019. doi: 10.26153/tsw/17286
[28]-Muratal, Onur, and Ridvan Yamanoglu. Production of 316l stainless steel used in biomedical applications by powder metallurgy. IEEE-Scientific Meeting on electrical-Electronics & biomedical engineering and Computer Science (EBBT), 1-4 (2019).
[29]-Wu MW, Huang ZK, Tseng CF, et al. Microstructures, mechanical properties, and fracture behaviors of metal-injection molded 17-4PH stainless steel. Met Mater, 21, 531–537 (2015).